2011 50th IEEE Conference on Decision and Control and
European Control Conference (CDC-ECC)
Orlando, FL, USA, December 12-15, 2011

Design and Analysis of an Image-based ACC Controller

Torsten Seyffarth

Abstract—**It is an important aim to reduce the cost of driver assistance systems to bring their benefit in safety and comfort to as many drivers as possible. A single camera used as an environmental sensor has the potential for a significant cost reduction. Based on the currently available camera and image processing technology this work evaluates how the portfolio of the camera based assistance systems can be expanded by an ACC function. By transferring the method of image-based controlling from robotic to distance control of vehicles, a known controller for radar systems is adapted to the characteristics of the camera. The detailed analysis of the resulting controller shows the influence of the controller parameters on different aspects of the system behavior.**

I. Introduction

Besides the individual tragedy traffic accidents with killed and injured people as well as property damage to vehicles and infrastructure cause a huge direct and indirect economic damage. These are the reasons why engineers, scientists and politicians [1] work on safety systems to reduce the number of accidents or to mitigate their consequences. In addition to the long known passive systems the active safety and advanced driver assistance systems (ADAS) make a contribution to achieve this aim [2].

But these systems can only help the driver if they are equipped in the car. To fulfill this in as many vehicles as possible the systems have to become as cheap as possible. The main cost factor of ADAS's is the environmental sensor. Therefore a single camera has the potential of a great cost reduction. First the basic technology is also used in other big mass markets like mobile phones or digital camcorders, so continuously decreasing prices can be expected. And second the sensor can be used for a lot of ADAS's like Lane Departure Warning, High Low Beam Control, Traffic Sign Detection and Forward Collision Warning. The buying incentive would be even more increased if the portfolio of the functions could be expanded by the comfort function ACC. This function gives the driver an advantage at all times and not only in critical situations which increases the value for the driver.

Current ACC Systems use mainly radar sensors or the fusion of this sensor with other sensor types. The advantage of the radar is the very precise measurement of distance, velocity and acceleration of the preceding vehicle, which are the most important input signals for the distance controller. In contrast to this the biggest disadvantage of the camera is providing exactly these signals [3]. In detail there are more differences between the two sensor types that effects the limits, availability and feeling of the function like lateral measurement accuracy or detection range. But this paper focuses on adapting the controller to the disadvantage of the camera at longitudinal measurement values to make an affordable ACC system with this sensor possible.

Human beings show every day that "ACC" is possible with a vision system only. Most people are using two "cameras" for this task, but also persons with a dysfunctional stereoscopic view can drive cars. And also for the rest the stereoscopic view is limited to the near field, although there are different opinions about the exact range [4], [5]. So this paper focuses on the cheaper mono camera system.

A basic requirement is an image processing system that detects the back of the preceding vehicles. The many existing different approaches for this task [6], [7] include algorithms based on detecting the vehicle edges, the symmetry of the vehicles, searching for elements like circles and methods from "machine learning". On the basis of this detection image- and position-based measurements are extracted [8], [9]. For this paper it is assumed, that an image processing system providing the signals distance, width and scale change of all vehicles as good as possible is given.

All currently known ACC controllers use the distance, velocity and some also the acceleration of the preceding vehicle for operating the host vehicle. For a camera based system this is called the position-based approach. Regardless of the sensor system there are five types of controllers in the literature, listed in the following with one example: fuzzy controller [10], cascade controller [11], model based controller [12], sliding mode controller [11] and finally controller based on modeling the human behavior [13].

Most of these position-based approaches were developed for radar based systems. Adapting ACC for the camera was done from the image processing point of view. The controller stayed the same and the aim was to provide the position-based signals with the camera as well as possible [8], [14].

In this paper the controller is adapted to the camera system by the image-based method to overcome the disadvantages of the longitudinal measurements of the camera and achieve an ACC result comparable to a radar sensor. The image-based method is originated in the robotic field [15]. The

T. Seyffarth works in the department Electrics/Electronics and Driver Experience Environment, BMW Group, Munich, Germany torsten.seyffarth@bmw.de

The author wants to thank Prof. G. Klinker and Prof. B. Lohmann for fruitful discussions and the support of his work.

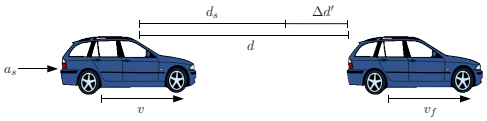

Fig. 1. Control problem

basic idea is to use values from the image space (here width and scale change) directly for the controller instead of signals transfered into the working space (here distance, velocity and acceleration). The higher effort in designing the controller and the loss of a general interface is the price for the reduction of calculation time and the absence of a position estimation and therefore of a geometrical model. Furthermore the controller are more robust against measurement noise, because the image signals are directly used.

The last aspect is the main focus of the controller in this paper. Other types of errors in input signals are latency, which could influence the stability of the controller (see section V-C), and an offset, which can not be compensated by the controller. An offset error has an effect on the function layer and must be taken into account there.

The image-based ACC controller is developed by first describing the control problem in detail. In section III a suitable position-based controller is chosen and converted to be used with image-based signals. Based on the construction method it has to be proven in section IV, that the controller problem is actually solved with the image-based controller. The influence of the controller parameters is analyzed in detail for different aspects in section V, before the paper closes in the last section with a short summary of the results and an outlook on future tasks.

II. Control Problem

For the description of the control problem and the controller design it is assumed, that the vehicle provides an acceleration interface towards the controller. For a lot of the current series cars this is already fulfilled. Otherwise solutions are known for providing such an interface [10], [11]. So for the further analysis $a \approx a_s$ can be assumed by neglecting the dynamic effects with the acceleration a of the host vehicle and the target acceleration a_s as the output of the ACC controller.

Figure 1 illustrates the following situation of an ACC vehicle. First the controller has to minimize the difference $\Delta d' = d - d_s$ between the actual distance d and the target distance d_s. In contrast to the usual definition here the distances between vehicles are defined from the camera position of the host vehicle to the rear of the preceding vehicle, to make the following equations easier to read. Because d and d_s are defined in the same way it has no effect on the behavior of the controller. The headway of a vehicle usually depends on the current velocity v, so the driver using an ACC system does not specify a constant distance but a time gap t_{d_w} towards the preceding vehicle. With the stand still distance d_0 the target distance is:

$$d_s = d_0 + t_{d_w}\, v = d_0 + t_{d_w}\, v_f - t_{d_w}\, v_r \qquad (1)$$

Second the controller has to bring the relative velocity $v_r = v_f - v$ between the host velocity v and the velocity of the preceding vehicle v_f as close to zero as possible. As additional constraint the velocity of the vehicle is not allowed to exceed the driver specified maximal velocity v_w.

III. Design of Image-Based Controller

For the design of the image-based controller the position-based cascade controller in [11] is used as the basis. The advantages towards the other known controller are that it already demonstrated its potential in the practical usage, it provides good opportunities for theoretical analyses of the controller and the mathematical model is not too complex which makes it not too reactive on signal noise.

[11] uses the distance d and the velocity of the preceding vehicle v_f as input signals of the environment in addition to the internal signals like the velocity of the host vehicle. For the image-based method the environmental signals must be replaced with signals from the image space. Because of the used image processing system the width of the vehicle in the image w in pixel is used to replace the distance. But all values that are inversely proportional to the distance can be used analogously like the height or the square root of the area. In the case of w the inversely proportional constant is $C = W \cdot f$ with the width of the vehicle W in meters and the focal length f in pixel.

In contrast to a radar system the camera cannot measure velocities directly, so a derivative has to be used. In this paper scale change ρ as a normalized, discrete derivative of w is used [8], but as above other similar signals can be used analogously. The only problem is, that $\rho = v_r/d$ is proportional to the relative velocity and not v_f. This has to be solved during the conversion of the position-based controller to an image-based one.

Before starting with this, the target width of the vehicle in the image w_s at d_s as command signal has to be calculated in a way that does not harm the image-based method. The relationship between the two signals is the following:

$$w_s = \frac{C}{d_s} = \frac{W\, f}{d_s} \qquad (2)$$

In general W is unknown and can vary a lot between the different types of vehicles e.g. motorcycles and trucks. But C can be calculated using $C = w \cdot d$ under the assumption, that the image processing system directly measures w and estimates d using other measurements. At first glance using d looks like a violation of the image-based method. But transforming the distance law (1) from the working space into the image space is not possible without a position-based signal. In the proposed way it is only used inside a product that is constant, so it can be filtered very strongly. In addition the distance is only used in the calculation of w_s, which can be filtered more than w and ρ without losing dynamic of the controller. So the aim of the new controller to prevent the

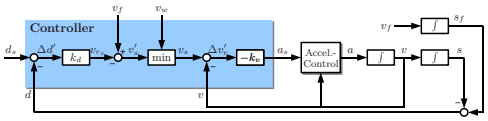

Fig. 2. Block diagram of the whole system with the position-based controller from [11] with the main input variable d, v_f and d_s. v_w is only needed for the side condition to limit the velocity by the drivers wish.

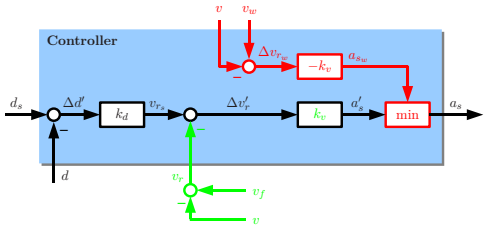

Fig. 3. By moving the minimum into the acceleration part and adding a copy of the velocity controller in parallel (red) the side condition can still be fulfilled but the velocity can be rearranged to get v_r as input for the distance controller (green).

noise of the position-based signal to influence the controller output is still fulfilled.

Figure 2 shows the block diagram of the whole system with the position-based controller from [11] with a different choice of some of the signatures. As described above the first aim is to achieve v_r as input signal. The reason for using v_f instead of v_r in [11] is to have v_s as intermediate result which can be limited with v_w to fulfill the additional constraint.

By adding a parallel velocity control as shown in figure 3 in red the minimum can be moved to the acceleration part. The minimum block can be interpreted as a switch choosing either the upper or the left path. The change of the controller is constructed to have the same result if the minimum blocks select the same way. In the first case the upper path is chosen if the following equation if fulfilled:

$$v_w < v_f - v_{r_s} \tag{3}$$

For the second case it is:

$$(v_w - v)\,(-k_v) < (v_f - v_{r_s} - v)\,(-k_v) \tag{4}$$

It can be seen that this is the same if $(-k_v) > 0$ is fulfilled. According to [11] this is true for a parameter choice that guarantees stability, if the differences in the signatures are taken into account. This way the velocity signals can be restructured and v_r can be defined as the input to the distance controller as shown in figure 3 in green.

Now the position-based signals can be exchanged by the image-based ones, which leads to a different system behavior and the following controller function:

$$a_s = k_\rho\, k_w\, (w_s - w) - k_\rho\, \rho \tag{5}$$

The resulting block diagram can be seen in figure 4. For investigation of the system behavior and comparison with the position-based controller the differential equation of the whole system in the working space is needed. Therefore the

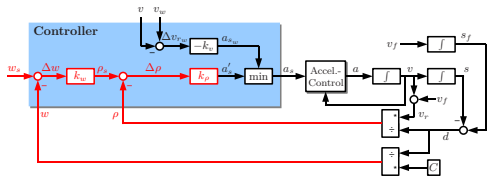

Fig. 4. After restructuring, all input signals that depend on the preceding vehicle can be replaced by image-based signals (red): $d \to w$, $d_s \to w_s$, $v_r \to \rho$. This is not an equivalent change, so the controller parameters are also different as well as the system behavior. The figure shows the block diagram of the whole system with the image-based controller.

output is transformed into the working space using $\rho = \dot{d}/d$ and $w = C/d$. Together with $\ddot{d} = \dot{v}_r = \dot{v}_f - a_s$ the differential equation of the system is:

$$\ddot{d} + k_\rho \frac{\dot{d}}{d} - k_\rho\, k_w\, C\, \frac{1}{d} = -k_\rho\, k_w\, C\, \frac{1}{d_s} + \dot{v}_f \tag{6}$$

For a better overview d_s is not replaced by (1) at this point. As a comparison the differential equation of the system with the position-based controller according to [11] but with the different signature choice of this paper is the following:

$$\ddot{d} - k_v\, \dot{d} - k_v\, k_d\, d = -k_v\, k_d\, d_s + \dot{v}_f \tag{7}$$

The two main differences of (6) and (7) are that the system behavior with the image-based controller is non-linear and depends on the preceding vehicle, because C appears in the formula. Normally it is not wanted that the system reacts differently e.g. with a preceding motorcycle or truck. Because C can be estimated like described above for calculating w_s, this behavior can be corrected by using a vehicle dependent controller parameter $k_w = k'_w/C$, with a new constant k'_w. This results in the following differential equation:

$$\ddot{d} + k_\rho \frac{\dot{d}}{d} - k_\rho\, k'_w\, \frac{1}{d} = -k_\rho\, k'_w\, \frac{1}{d_s} + \dot{v}_f \tag{8}$$

There are ways to get a linear system behavior e.g. with other input variables, not constant gain parameters or the method of "exact linearization". But all of them lead to the same result as the position-based controller and harm the image-based method by either needing position-based signals directly inside the controller or by not directly using the image-based signals. In the end the non-linearity is not a disadvantage of the controller but shows its adaption to the characteristic of the camera system.

IV. Stability Analysis

The controller design above ensures the image-based method and the limitation of v to v_w but not the solution of the control problem. To prove this, first the stationary states are calculated and then the stability of these states are investigated.

For calculating the stationary states the differential equation of the velocity is needed. For this (8) is differentiated with respect to time and with $\dot{d} = v_f - v$ we get:

$$\ddot{v} + k_\rho \frac{\dot{v}}{d} + k_\rho \frac{(v_f - v)^2}{d^2} + k_\rho k'_w \frac{v}{d^2} = k_\rho \frac{\dot{v}_f}{d} + k_\rho k'_w \frac{v_f}{d^2} - k_\rho k'_w \frac{\dot{d}_s}{{d_s}^2} \quad (9)$$

In the stationary state all derived variables are set to zero ($\ddot{v} = \dot{v} = \dot{v}_f = \dot{d}_s = 0$). There are two solutions for the velocity in the obtained equation:

$$v_1 = v_f \Rightarrow v_r = \dot{d} = 0 \quad (10)$$

$$v_2 = v_f - k'_w \Rightarrow v_r = \dot{d} = k'_w \quad (11)$$

These two velocities are set into (8) together with all derived variables set to zero. For v_1 the stationary distance is $d = d_s$. For v_2 the solution of the equation is $0 = 1/d_s$, which is not solvable with $d_s \in \mathbb{R}$. So the only valid stationary state is:

$$\begin{pmatrix} d \\ v_r \end{pmatrix}_R = \begin{pmatrix} d_R \\ v_{r_R} \end{pmatrix} = \begin{pmatrix} d_s \\ 0 \end{pmatrix} \quad (12)$$

This is exactly the aim of the controller according to the specified control problem. But for the solution it is also important to reach this stationary state so that the system behavior is stable. For investigating the stability of the system it is assumed that $\dot{v}_f = 0$ is fulfilled, otherwise the stationary state is not constant. And for the dynamic behavior the chosen distance law (1) is relevant.

The system behavior is represented by a non-linear differential equation of order 2. So all methods for analyzing the stability which require linearity can't be used here. In addition an analytical solution is not possible even if the order is reduced to 1 by eliminating the time as described in [16].

Therefore two approximation methods are used. The first one deduces information of the system behavior from the trajectories in the phase plane [16], which is only possible for a system of order 2. This way the results of the second method can be visualized, too. The method is linearizing the non-linear differential equation.

For the calculation of the trajectories in the phase plane the differential equation of order 2 is converted to a system of two differential equations of order 1. In addition the dynamic variables are changed to the deviation of the stationary state. In this shape the equation can be solved numerically for different start conditions. The start conditions of the problem can be limited by their practical relevance to a maximal relative velocity of $\pm 60\ km/h$ and a maximal range of $100\ m$. The resulting trajectories for $v_f = 65\ km/h$ can be seen in figure 5 in blue. All trajectories end in the stationary state, so the system behavior is asymptotically stable for this choice of the controller parameters.

This method gives a good overview of the system behavior for one parameter choice. For general information like which parameter values are stable the linearization is more suitable, because this way analytical investigations are possible. For the linearization a Taylor expansion in the stationary state is used:

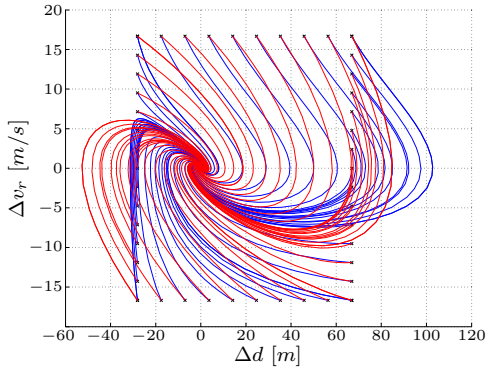

Fig. 5. Trajectories of the system state in the phase plane (blue = system with image-based controller, red = linearized equations of the system with image-based controller)

$$\Delta\ddot{d} + \underbrace{\left(\frac{k_\rho k'_w t_{d_w}}{(d_0 + t_{d_w} v_f)^2} + \frac{k_\rho}{d_0 + t_{d_w} v_f} \right)}_{b_1} \Delta\dot{d} + \underbrace{\frac{k_\rho k'_w}{(d_0 + t_{d_w} v_f)^2}}_{b_0} \Delta d = 0 \quad (13)$$

The trajectories of the linearized system are also shown in figure 5 in red. Especially further away from the stationary state the trajectories are much different, but at the end they come close together again. Overall the behavior is a similar stable vortex as for the original differential equation. This indicates that the results based on the linearized equation are a good approximation for the original system.

The stability of a homogeneous, linear differential equation can be derived from the roots of its characteristical polynomial [16]. So the following results are deduced:

$$\forall k_\rho, k'_w\text{: } k_\rho > 0 \wedge k'_w > 0 \Rightarrow \quad \text{stable} \quad (14)$$

$$\forall k_\rho, k'_w\text{: } k_\rho \cdot k'_w < 0 \quad \Rightarrow \text{not stable} \quad (15)$$

$$\exists k_\rho, k'_w\text{: } k_\rho < 0 \wedge k'_w < 0 \Rightarrow \quad \text{stable} \quad (16)$$

There are negative parameters with a stable system behavior but with these parameters the system is oscillating so much, that they have no practical relevance. So only positive parameters are further investigated. According to [16] two behaviors of the stable system are possible. First the above shown vortex behavior noticeable at the logarithmic helix of the trajectories. Second a node behavior with trajectories running into the stationary state at linear asymptotes. The next section investigates, how the controller parameters have to be chosen to achieve one or the other system behavior.

V. Theoretical Analysis

A. System Behavior

For the comfort of the passengers the node behavior is more convenient, because the oscillations could be very

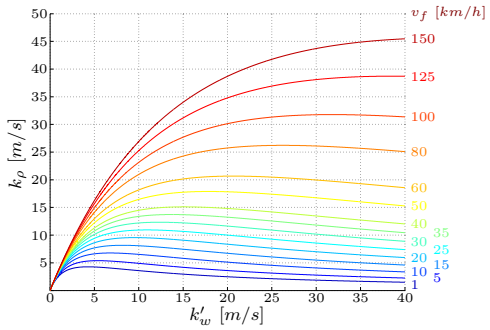

Fig. 6. Boundary of the parameter choice for node behavior (node behavior is above the curves)

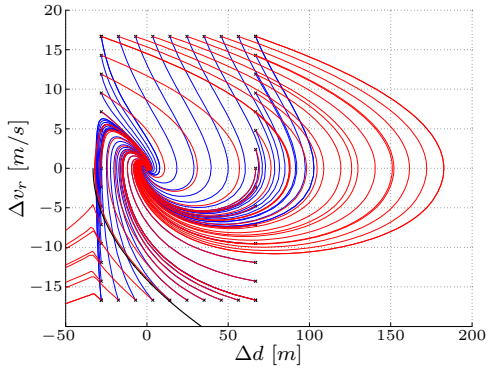

Fig. 7. System behavior with limited actuating variable (blue = unlimited, red = limited, black = limitation of the adjustable area)

unpleasing especially at constant following situations. As for the stability the type of behavior can be derived from the roots of the characteristical polynomial of the linearized differential equation. So for $k_\rho > 0 \wedge k'_w > 0$ node behavior is obtained if $b_1^2 - 4\,b_0 \geq 0$ and vertex behavior otherwise. Therefore for node behavior the two controller gains have to fulfill the following constraint:

$$\begin{aligned} 0 &\leq b_1^2 - 4\,b_0 \\ \Leftrightarrow k_\rho &\geq \frac{4\,k'_w\,d_R^2}{(k'_w\,t_{d_w} + d_R)^2} \end{aligned} \tag{17}$$

$$\Rightarrow k'_w \begin{cases} \text{arbitrary}, & \text{if } d_R - k_\rho\,t_{d_w} < 0, \text{ otherwise} \\ \geq \frac{d_R}{k_\rho\,t_{d_w}^2}\cdot & (2\,d_R - k_\rho\,t_{d_w} \\ & \quad + 2\,\sqrt{d_R}\,\sqrt{d_R - k_\rho\,t_{d_w}}) \vee \\ \leq \frac{d_R}{k_\rho\,t_{d_w}^2}\cdot & (2\,d_R - k_\rho\,t_{d_w} \\ & \quad - 2\,\sqrt{d_R}\,\sqrt{d_R - k_\rho\,t_{d_w}}) \end{cases}$$

Otherwise the system has a vortex behavior. The first important investigation is, that the constraint depends on d_R and therefore on v_f. Hence the system can have different behaviors for various velocities of the preceding vehicle. That is why figure 6 shows the result of (17) for equality regarding different v_f. Vortex behavior is below the lines.

From the inequations and the figure some easier rules for the controller gains can be approximated. For a given k'_w the parameter k_ρ has to be increased to come closer to the node behavior. It is the same for the velocity of the preceding vehicle. For a given use case the maximal velocity of the preceding vehicle determines the choice of k_ρ. Increasing the parameter means the controller reacts harder to deviation from the stationary state.

Below a certain v_f which depends on k_ρ the choice of k'_w is arbitrary. The system has always a node behavior. For higher velocities and a given k_ρ the parameter k'_w must be decreased to come closer to the node behavior. Theoretically there are also very high values for k'_w possible, but these have no practical use. Decreasing k'_w means that the distance error is weighed less and the system behavior approaches a purely velocity control.

This way an arbitrary number of parameters for a node behavior can be found. But there are additional constraints that must be fulfilled for the practical use of the controller. These constraints lead to different requirements which are partly contrary. In the following the constraints are investigated to show how the controller parameters have to be changed to fulfill a certain property. Depending on the way the producer weights the requirements the gains can be chosen accordingly.

B. Limited Acceleration

The first investigated issue is that in the practical system the allowed acceleration and deceleration of the controller is limited, to make the system controllable by the driver in case of a fault reaction. As an example $a_{min} = -3m/s^2$ and $a_{max} = 1.2m/s^2$ is used here. This limitation can be integrated in the numerical calculation of the trajectories as shown in figure 7. It can be seen that the difference between the original, blue trajectories and the limited, red ones are bigger in the upper half, because the absolute value of a_{max} is smaller. The form of the trajectories is a bigger arc because the controller needs more time to achieve the higher velocity of the preceding vehicle.

But even worse is that some trajectories in the lower left corner do not end in the stationary state but depart from it unlimited. This is caused by the limitation of the controller, so that the initial relative velocity can't be reduced until the preceding vehicle is behind the image plane. This does not mean that the controller is not stable, but that for a initial relative velocity of $v_r(0)$ a certain initial distance d_{min} is needed to prevent the accident with a limited deceleration. This initial distance can be obtained for $v_r(0) \leq 0$ from the motion equations for a linear motion with constant acceleration:

$$\Delta d_{min} = -d_R - 1/2\,\frac{\Delta v_r(0)^2}{a_{min}} \tag{18}$$

This boundary can be seen in figure 7 as a black line. For smaller distances the trajectory will not end in the stationary state, but it has to be proven, that for larger or equal values the controller keeps stable. For this it has to be verified, that a trajectory from the right side never crosses

this boundary. And for this again it is sufficient and necessary to show that all states of the unlimited controller lead to an acceleration smaller or equal than a_{min} (higher or equal absolute value), because this way the trajectory will exactly follow the boundary and reach the stationary state at the end. Otherwise the trajectory would cross the boundary and proceed behind the image plane. Because two trajectories are identical if they are identical in one point, it is enough to show that the requirement $a \leq a_{min}$ is fulfilled on the boundary for $t = 0$. This way the differential equation becomes a normal equation. So with $d = \Delta d + d_R$, $t = 0$, $\Delta\dot{d}(0) = \Delta v_r(0)$, $\Delta\ddot{d} = \dot{v}_f - \dot{v} = -a$, $\Delta d(0) = \Delta d_{min}$ and (1) in (8) the following is obtained:

$$a = -2\,k_\rho\,\frac{|a_{min}|}{|\Delta v_r(0)|} - 2\,k_\rho\,k'_w\,\frac{|a_{min}|}{|\Delta v_r(0)|^2} + k_\rho\,k'_w\,\frac{1}{d_R + t_{d_w}\,|\Delta v_r(0)|} \tag{19}$$

For an easier analysis $a_{min} = -|a_{min}|$ and $\Delta v_r(0) = -|\Delta v_r(0)|$ are replaced in the formula, showing that both values are negative. $a \leq a_{min}$ is supposed to be for all $0 < \Delta v_r(0) \leq \Delta v_{rl}$, with Δv_{rl} the lower boundary of the relative velocity used in the phase plane. For $|\Delta v_r(0)| \to 0$ the negative terms of the function are dominant and the acceleration goes to $-\infty$. The larger $|\Delta v_r(0)|$ gets the more the absolute values for each term decrease and the positive term gets more dominant, so that the acceleration increases continuously. Therefore the requirement is fulfilled for all $\Delta v_r(0)$ in the inspected range, if it is fulfilled for $\Delta v_r(0) = \Delta v_{rl}$. This leads to the final requirement for the controller gains:

$$k_\rho \geq \frac{|a_{min}|}{\frac{2\,|a_{min}|}{|\Delta v_{rl}|} + k'_w\left(\frac{2\,|a_{min}|}{|\Delta v_{rl}|^2} - \frac{1}{d_R + t_{d_w}\,|\Delta v_{rl}|}\right)} \tag{20}$$

$$\Leftrightarrow k'_w \geq \frac{|a_{min}|}{k_\rho\,\frac{2\,|a_{min}|}{|\Delta v_{rl}|^2} - k_\rho\,\frac{1}{d_R + t_{d_w}\,|\Delta v_{rl}|}} + \frac{\frac{2\,|a_{min}|}{|\Delta v_{rl}|}}{-\frac{2\,|a_{min}|}{|\Delta v_{rl}|^2} + \frac{1}{d_R + t_{d_w}\,|\Delta v_{rl}|}} \tag{21}$$

So the controller parameter must have a certain minimum value to guarantee stability in the whole restricted area. The larger one parameter is the smaller the other can be chosen.

C. Latency

Another issue in the real vehicle are latencies and delays, which are approximated by latencies here. These can be caused by different sources. E.g. the engine or the brake need time to react on a change of the target moments or there is a latency in the signals of the image processing. These latencies can vary in different situations, so that the calculation will be based on a worst case estimation T_t. The negative effect of the latency is, that the system behavior can become unstable because of the postponed reaction.

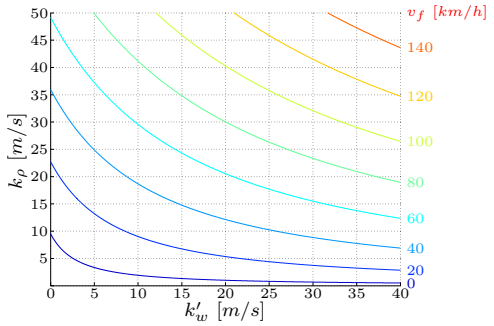

Fig. 8. Boundary of the parameter choice for stability with latency (unstable behavior is right above the curves)

For the analysis of the effect of latencies it is helpful to switch to the discrete representation. This way the latency can be modeled as a shift of the sampling instances. The controller in modern vehicles is usually implemented on an electronic control unit which perfectly fits to a discrete representation. And with a sampling time of $T = 0.02s$ it is quasi continuous which is sufficient to represent the rest of the system. Therefore continuous and discrete representation are equivalent in this case.

For the discretization of the differential equation the differential quotients are replaced by backward difference quotients [17]. In the following the abbreviation $\Delta d_j = \Delta d(j * T)$ with $j \in \mathbb{N}$ is used. The considered latencies have different sources in the control loop but in the end the same impact. The current state change is not based on the current state but on the one T_t seconds ago. So the latency can be put in the formula to the controller output. In the specific terms j is replaced with $j' = j - j_t$ with $j_t = T_t/T$, assuming that T_t is an integer multiple of T. Because there is an analytic approach to inspect the stability, the linearized differential equation 13 is discretized and brought into the standard form of difference equations:

$$\Delta d_j - 2\,\Delta d_{j-1} + \Delta d_{j-2} + (T\,b_1 + T^2\,b_0)\,\Delta d_{j'} - T\,b_1\,\Delta d_{j'-1} = 0 \tag{22}$$

According to [17] this is stable exactly if the roots of the following polynomial are inside of the unit circle in the complex plane:

$$z^{j_t+1} - 2\,z^{j_t} + z^{j_t-1} + (T\,b_1 + T^2\,b_0)\,z - T\,b_1 = 0 \tag{23}$$

With increasing latency the order of the polynomial increases, too. For $j_t \geq 4$ the polynomial is not analytically solvable anymore. But for the analysis of the stability the actual roots are not needed, only if they are inside the unit circle. According to [18] there are analytical methods to decide this directly by the coefficients of the polynomial. But for (23) the necessary criteria are not meaningful enough and the sufficient criteria do not lead to manageable formulas. So the roots have to be calculated numerically to find the requirement for stability.

Normally the latency is known and the requirements for the parameters are needed to guarantee stability. The result for the boundary of the two parameters is shown in figure 8 for different target velocities and with a latency of $T_t = 1s$. To the top right of the boundary the system behavior is instable. Hence this is an upper limit for the controller gains. The smaller one parameter is the larger the other can be chosen. In the practical usage the boundary should not be exhausted because before the system becomes instable it already starts to oscillate heavily.

D. Transient Time

In addition to stability the practical system should reduce a deviation in the distance or velocity in a sufficient time. This means not too slow so that the driver deactivates the system because it reacts not enough and not too fast so that it becomes inconvenient for the passengers. Where exactly the boundaries are is a decision of the producer for its costumers.

For the analysis of the relationship between the transient time and the controller gains the function of the distance error is approximated with the linearized differential equation (13) and examined for a specific start condition. The transient time is defined here by the time until the distance error is finally below a threshold of $\Delta d_g = 1m$. This is only possible if the velocity error is also limited, so this will not be investigated explicitly.

As start position $\Delta d(0) = -d_R + 5$ is used. This is the lower limit for the distance in the phase plane and very near to the host vehicle. For small target velocities the upper limit would be a larger deviation in absolute numbers. But for a better comparability on the results the possibility of different start positions depending of the target velocity is not used. The velocity error is in the beginning $\Delta\dot{d}(0) = 0$. This makes the calculation easier without harming the results.

The linearized differential equation (13) is a linear differential equation of the order 2. The analytic solution depends on the roots of the characteristic polynomial $\lambda^2 + b_1\,\lambda + b_0$. Therefore the solution for the function of the distance error is separated into three cases:

$$\Delta d(t) = \Delta d(0)\, e^{pt} \left(-\frac{p}{q} \sin(qt) + \cos(qt) \right),\ c < 0 \quad (24)$$

$$\Delta d(t) = \frac{\Delta d(0)}{\lambda_2 - \lambda_1} \left(\lambda_2 e^{\lambda_1\, t} - \lambda_1 e^{\lambda_2\, t} \right),\ c > 0 \quad (25)$$

$$\Delta d(t) = \Delta d(0)\, e^{\lambda\, t} \left(1 + \frac{b_1}{2}\, t \right),\ c = 0 \quad (26)$$

$$\text{with } p = -\frac{b_1}{2}\ ;\ q = \sqrt{b_0 - \frac{b_1^2}{4}}\ ;\ c = \frac{b_1^2}{4} - b_0$$

$$\lambda_{1,2} = -\frac{b_1}{2} \pm \sqrt{\frac{b_1^2}{4} - b_0}\ ;\ \lambda = -\frac{b_1}{2}$$

In this separation the node (case 2 and 3) and vortex (case 1) behavior can be found. For the first two cases the equations can be solved for t in a good approximation by applying $\Delta d(t) = \Delta d_g$. In the first case the damped oscillation can be approximated by the enveloping exponential function. So in both cases the function is finally below Δd_g when it reaches this value for the first time. So t equals the transient time t_a:

$$t_a = ln \left(\frac{\Delta d_g}{\Delta d(0)}\, \frac{\sqrt{b_0 - \frac{b_1^2}{4}}}{\sqrt{b_0}} \right) \frac{-2}{b_1},\ \text{for } c < 0 \quad (27)$$

$$t_a = ln \left(\frac{\Delta d_g}{\Delta d(0)}\, \frac{\lambda_2 - \lambda_1}{\lambda_2} \right) / \lambda_1,\ \text{for } c > 0 \quad (28)$$

The third case applies only for one discrete value of the discriminant. It is solved numerical because there is no analytic solution and no suitable approximation for this case was found.

Figure 9 illustrates the results for the two controller variables with different target velocities. The discrete case is marked with "+" and the second case is separated from the first by the dotted line. In the area of the root of the discriminant the approximation of the second case becomes inaccurate. The graph has to go further in the direction of the "+". The function for the first case is a worst case approximation. Depending on the exact behavior of the oscillation the error drops below the threshold before time t_a. But then the graph becomes discontinuously, which depends on many factors. So for the application this approximated function is more suitable.

Overall it can be summarized that for increasing k'_w the transient time becomes smaller but with a decreasing rate. For k_ρ the behavior is similar until approximately to the root of the discriminant. After that the transient time slightly increases. Overall the transient time cannot fall below a certain value.

E. Measurement Errors

The final issue that is investigated is the effect of measurement errors. Latency is already discussed. This leaves measurement noise and offset. The last one only occurs for the distance d and the width in the image w.

For d the measurement noise can be neglected for the image-based controller because it is only used in a highly filtered version for the calculation of w_s. But an offset has a noticeable effect. The controller reacts on the preceding vehicle in a way that d equals d_s is reached. If there is a constant offset on d towards the real distance, the controller results differ from d_s by the same amount. There is no possibility for the controller to avoid this error assuming that the image processing already uses all possible information to provide the best distance estimation.

For w the effect of the error is the other way around. An offset error has no effect as long as it is constant. For the controller the vehicle appears just a little bit bigger or smaller than it is. With the use of the vehicle depending controller gain this has no effect on the system behavior. On the other hand measurement noise on w has a noticeable effect on the noise of the controller output. For ρ the effect of measurement noise is the same.

How much the noise on these input signals effects the noise on the controller output depends on the value of the

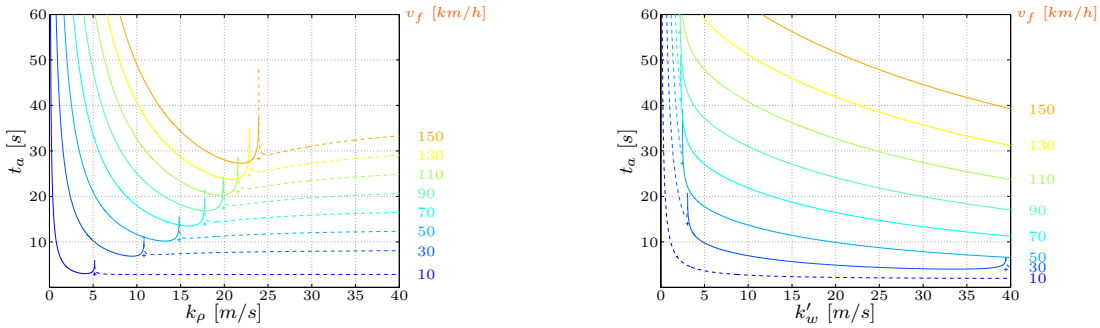

(a) With respect to k_ρ

(b) With respect to k'_w

Fig. 9. Transient time for equation (26) with +, (27) with solid line and (28) with dashed line

controller parameters. The noise can be modeled here by average free Gaussian noise neglecting other types of errors like latency and offset. So it is completely described by the variance of the signal. Because the controller law is linear the resulting variance can be calculated from the input variances. The variance of the target acceleration V_{a_s} is as follows with $V_w = \mathrm{Var}(w)$ and $V_\rho = \mathrm{Var}(\rho)$:

$$V_{a_s} = k_\rho^2 \left({k_w}^2 \, V_w + V_\rho + 2 \, k_w \, \sqrt{V_w \, V_\rho} \, \mathrm{Co}(w, \rho) \right) \quad (29)$$

It can be seen that the variance of the controller output increases with the square of the controller gains. Especially higher values for k_ρ have a negative effect, because it is a factor for all variances. So in situations, in which the noise is most noticeable like constant following, the parameters have to be chosen as small as possible. In addition it has to be considered, that in the formula k_w appears and not k'_w. The value of k_w increases with the width of the target vehicle so the widest vehicles like trucks have to be taken into account when V_{a_s} is calculated.

VI. Conclusion

This paper presents a novel approach for a camera based ACC controller. A known ACC cascade controller is changed in a way, that image-based signals can be directly used as input for the controller. A position-based signal is only needed in a highly filtered version for calculating the target value. It is proven that the designed controller solves the control problem and that it is globally, asymptotically stable for all positive controller gains.

Furthermore the influence of the controller parameters on the system behavior is investigated to achieve different results. It is shown that the effects of limited acceleration, latency, transient time and measurement errors create rules and boundaries for the parameter choice. This way the controller can be adapted for different use cases according to the wishes of the producers and costumers.

Future research on controller side will have to compare the image-based and position-based controller practically, to investigate if the image-based controller shows the expected improvements. In addition no controller can deal with certain typical errors of the image processing like offset or missed detections. So adaption on the function level has to be taken into account to address these as well as a better integration of the different functions and information available with a camera sensor.

References

[1] Anonym, *Weißbuch: Die europäische Verkehrspolitik bis 2010: Weichenstellungen für die Zukunft*. Luxemburg: Amt für Amtliche Veröff. der Europ. Gemeinschaften, 2001.

[2] R. Freymann, "Möglichkeiten und grenzen von fahrerassistenz- und aktiven sicherheitssystemen," in *Akt. Sicherheit durch FAS*. Tagung des Lehrstuhls für Fahrzeugtechnik der TU München, 2004.

[3] D. Wisselmann, K. Gresser, H. Spannheimer, K. Bengler, and A. Huesmann, "Connecteddrive - ein methodischer ansatz für die entwicklung zukünftiger fahrerassistenzsysteme," in *Akt. Sicherheit durch FAS*. Tagung des Lehrstuhls für Fahrzeugtechnik der TU München, 2004.

[4] K. D. Mörike and E. Betz, *Biologie des Menschen*, 15th ed. Hamburg: Nikol, 2007.

[5] R. Klinke, H.-C. Pape, A. Kurtz, S. Silbernagl, R. Baumann, B. Brenner, R. Gay, and A. Rothenburger, *Physiologie*, 6th ed. Stuttgart: Thieme, 2010.

[6] M. Bertozzi, A. Broggi, M. Cellario, A. Fascioli, P. Lombardi, and M. Porta, "Artificial vision in road vehicles," *Proc. of the IEEE*, vol. 90, no. 7, pp. 1258–1271, 2002.

[7] I. Masaki, *Vision based vehicle guidance*. New York: Springer, 1992.

[8] G. P. Stein, O. Mano, and A. Shashua, "Vision-based acc with a single camera: bounds on range and range rate accuracy," in *IVS*, 2003, pp. 120–125.

[9] R. Aufrere, F. Marmoiton, R. Chapuis, F. Collange, and J. P. Derutin, "Road detection and vehicle tracking by vision for adaptive cruise control," *Int. j. of robotics research*, vol. 20, no. 4, pp. 267–286, 2001.

[10] S. Germann, *Modellbildung und modellgestützte Regelung der Fahrzeuglängsdynamik*. Düsseldorf: VDI-Verlag, 1997.

[11] K. Naab, "Geschwindigkeits- und abstandsregler," in *Seminar "Abstandsregelung"*. Haus der Technik E.V., 1999.

[12] L. Bin, W. Rongben, and C. Jiangwei, "A new optimal controller for intelligent vehicle distance," in *IVS*, 2002.

[13] M. Canale and M. Stefano, "Tuning of stop and go driving control strategies using driver behaviour analysis," in *IVS*, 2002.

[14] M. A. Sotelo, D. Fernandez, J. E. Naranjo, C. Gonzalez, R. Garcia, T. de Pedro, and J. Reviejo, "Vision-based adaptive cruise control for intelligent road vehicles," in *IROS*, 2004, pp. 64–69.

[15] P. I. Corke, S. A. Hutchinson, and G. D. Hager, "A tutorial on visual servo control," *T-RA*, vol. 12, no. 5, pp. 651–670, 1996.

[16] O. Föllinger, *Nichtlineare Regelung I*. München: Oldenbourg, 1993.

[17] H. Unbehauen, *Regelungstechnik II*. Braunschweig: Vieweg, 2000.

[18] O. Föllinger, *Lineare Abtastsysteme*. München: Oldenbourg, 1993.